Journal of Hazardous Materials 193 (2011) 325–329

Contents lists available at ScienceDirect

Journal of Hazardous Materials

journal homepage: www.elsevier.com/locate/jhazmat

Short communication

Novel magnetic Fe_3O_4@C nanoparticles as adsorbents for removal of organic dyes from aqueous solution

Zhengyong Zhang, Jilie Kong*

Department of Chemistry, Fudan University, Shanghai 200433, China

ARTICLE INFO

Article history:
Received 4 November 2010
Received in revised form 7 July 2011
Accepted 7 July 2011
Available online 2 August 2011

Keywords:
Magnetic separation
Fe_3O_4/C
Adsorption
Methylene blue
Cresol red

ABSTRACT

The magnetic Fe_3O_4/C core–shell nanoparticles have been synthesized by a simple strategy and used as adsorbents for removal of organic dyes from aqueous solution. The resulting products are characterized by scanning electron microscope (SEM), energy dispersive X-ray spectrometry (EDX), X-ray photoelectron spectroscopy (XPS), X-ray diffraction (XRD), Raman spectra and Fourier transform infrared spectra (FTIR). Adsorption performances of the nanomaterial adsorbents are tested with removal of methylene blue (MB) and cresol red (CR) from aqueous solution. The effects of solution pH value, adsorption time and capacity of the nanocomposites have been fully investigated. The results reveal that the nanospheres can be easily manipulated by an external magnetic field with high separation efficiency. In addition, the process is clean and safe for purifying water pollution. The prepared Fe_3O_4/C complex nanomaterials could thus be used as promising adsorbents for the remove organic dyes, especially, cationic dye, from polluted water.

1. Introduction

Organic dyes are widely used in various fields and seriously induce water pollution. Most of the industrial dyes are toxic, carcinogenic, and teratogenic [1] and unfortunately most of them are stable and resistance to photo degradation, biodegradation, oxidizing agents [2]. Conventional physicochemical and biological treatment methods are ineffective for removal these dyes due to their extreme stability. Hence, adsorption technique becomes one of the preferable choices to purify the waste water which containing dyes.

Recently, magnetic loaded adsorbent materials have gained special attention in water purification [3], based on their numerous advantages such as high separation efficiency, simple manipulation process, kind operation conditions [4] and easy specifically functional modifications. Gong et al. prepared magnetic multiwall carbon nanotube nanocomposite as an adsorbent for removal of cationic dyes from aqueous solution [5]. Ai et al. and Luo et al. reported that the magnetic composites with activated carbon could efficiently adsorb organic dyes [6,7], respectively. Zargar et al. reported that iron oxide nanoparticles coated with cetyltrimethylammonium bromide (CTAB) performed as a high efficient adsorbent for removal of amaranth (AM) from water solution [8]. While Elwakeel and Zhu et al. found that when the iron oxide nanoparticles cross-linked with chitosan, the removal ability to reactive black 5 and hazardous azo dye were greatly improved [9,10]. Other magnetic particles, including magnetic silica modified with amine groups and magnetic alginate beads cross-linked with epichlorohydrin, were found adsorb acid orange 10 [11] and similar dyes [12,13] with high efficiency. However, little study is done on adsorption of dyes by magnetic particles cross-linked with carbon until now, which is easily synthesized, particularly economic and environment friendly.

In this work, using $FeCl_3{\cdot}6H_2O$ as an iron source and glucose as a carbon source, novel superparamagnetic Fe_3O_4/C core–shell nanoparticels were prepared as adsorbents for removal of organic dyes from aqueous solution. The composites displayed high efficiency to adsorb contaminants from aqueous effluents. And after adsorption accomplished, they can be easily separated from the water by an adscititious magnetic field. The adsorption kinetics was fully investigated and two typical dyes, methylene blue (MB) and cresol red (CR), were employed as model organic pollutants to test the adsorption performance of the nanoparticles.

2. Experimental

2.1. Materials and methods

Ferric trichloride ($FeCl_3{\cdot}6H_2O$), sodium acetate anhydrous were obtained from Shanghai Wenming Biochemical Science & Technology Co., Ltd (Shanghai, China). Glucose, sodium hydroxide, concentrated nitric acid were purchased from Sinopharm Chemical Reagent Co., Ltd (Shanghai, China). Ethylene glycol was bought from Shanghai Qiangshun Chemical Reagent Co., Ltd (Shanghai, China).

* Corresponding author. Tel.: +86 21 65642138; fax: +86 21 65641740.
E-mail address: jlkong@fudan.edu.cn (J. Kong).

0304-3894/$ – see front matter © 2011 Elsevier B.V. All rights reserved.
doi:10.1016/j.jhazmat.2011.07.033

Methylene blue and cresol red were bought from Shanghai Chemical Reagent NO. 3 Co., Ltd (Shanghai, China). All chemicals used in this study were analytical grade. Double distilled water was used throughout.

Scanning electron microscope (SEM) micrograph of sample was taken using a Philips XL 30 electron microscope (Philips, Holland) with an accelerating voltage of 20 kV. Energy dispersive X-ray (EDX) spectrometry was carried out with spectroscope (Oxford, INCA) attached to SEM. X-ray diffraction (XRD) measurement was performed on a Bruker Advance 8 (Germany). X-ray diffractometer using Cu Kα radiation (λ = 0.1524 nm) from 20° to 70° (2θ). An infrared spectra analyzed was obtained from FTIR (Fourier Transform Infrared Spectrometer, Nicolet, Avatar-360, USA). The Raman spectrum image was measured by Raman spectrometer (λ = 632.8 nm, Labram-1B, Dilor Co., France). Ultraviolet–visual adsorption spectra measurements were from UV–vis absorption spectrometer (HP8453, USA). XPS experiments were carried out on a RBD upgraded PHI-5000C ESCA system (Perkin Elmer) with Mg Kα radiation ($h\nu$ = 1253.6 eV) or Al Kα radiation ($h\nu$ = 1486.6 eV). In general, the X-ray anode was run at 250 W and the high voltage was kept at 14.0 kV with a detection angle at 54°.

2.2. Preparation of Fe_3O_4 nanospheres

The preparation of magnetic nanoparticles was based on the previously reported procedures [14,15]. Briefly, $FeCl_3{\cdot}6H_2O$ (1.35 g), ethylene glycol (40 mL) were mixed and stirred period of time until $FeCl_3$ complete dissolution, then sodium acetate anhydrous (3.6 g) was added and reacted vigorously to acquire a transparent solution. Then the mixture was transferred to a Teflon-sealed autoclave at 200 °C for 8–16 h. The obtained products were cooled naturally, and washed several times with hot water and ethanol. Finally, dried at 60 °C, stand by to application.

2.3. Synthesis of Fe_3O_4/C nanoparticles

The synthesis method was referring to some reported work [16,17]. In brief, as-prepared Fe_3O_4 (200 mg) nanoparticles were dispersed in a 0.1 mol L^{-1} HNO_3 solution for 10 min, then followed by washing with deionized water several times. Subsequently, the treated magnetic nanospheres were dispersed in 0.5 mol L^{-1} glucose solution (20 mL) under vigorous stirring. After stirring for another 10 min, the solution was transferred to a Teflon-sealed autoclave and kept at 180 °C for 8–16 h then cooled naturally. The obtained products were separated by a magnet and washed several times with deionized water and ethanol. At last, they will be dried at 60 °C for future use.

2.4. Adsorption experiments

The experiments were carried out in glass bottles at room temperature. 5 mL of organic dyes solution of known initial concentration was shaked with different mass magnetic composites and different reaction conditions on a shaker at 250 rpm. The initial pH value of the dye solutions were adjusted with 0.1 mol L^{-1} HNO_3 or 0.1 mol L^{-1} NaOH solution using a pH meter. After magnetic separation using an external magnet, the equilibrium concentrations of dyes were measured with UV–vis spectrophotometer at appropriate wavelengths corresponding to the maximum absorbance of each dyes, 663 nm and 433 nm for MB and CR, respectively. Using the Lambert–Beer law as listed below and matching their absorption maximum to a predetermined standard curve of MB and CR, respectively, the final concentration of the dyes in solution can be calculated:

$$A = \epsilon bc$$

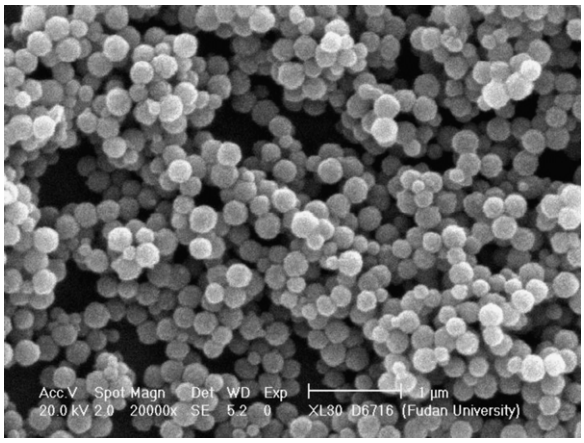

Fig. 1. SEM image of Fe_3O_4/C nanospheres.

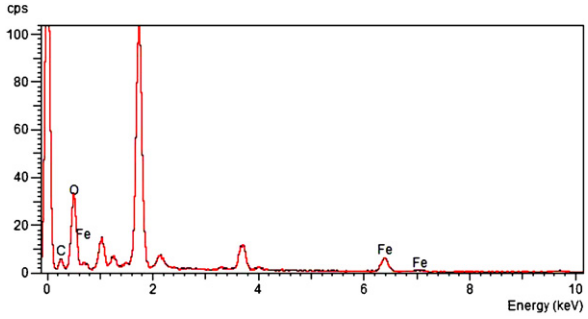

Fig. 2. EDX spectrum of Fe_3O_4/C nanoparticles.

where A is the absorbance, ϵ is the absorptivity, b is the optical distance, and c is the solution concentration.

3. Results and discussion

3.1. Synthesis and characterization of the Fe_3O_4/C nanospheres

Using a two-step synthesis route for the preparation of Fe_3O_4/C nanospheres, we prepared magnetic nanoparticles coated with carbon. Firstly, using $FeCl_3$ as an iron source, and ethylene glycol as both solvent and reductant, Fe_3O_4 magnetic nanospheres were obtained. Subsequently, the magnetic nanospheres were coated with a layer of carbon using glucose as a carbon source. After hydrothermal reaction with glucose, the Fe_3O_4 particles were modified with a hydrophilic carbonaceous layer. SEM image in Fig. 1 demonstrates that the prepared Fe_3O_4/C nanomaterials are spherical, narrowly distributed, and well dispersed, with average size about 250 nm in the diameter. The chemical composition of the nanoparticles was analyzed by EDX. The EDX spectrum (Fig. 2) shows iron, oxygen and carbon. It reveals that the iron was from magnetic Fe_3O_4, and carbon was from glucose production reacted. The nanomaterial was further confirmed and quantitative analysis by XPS, as shown in Fig. 3. From the distribution of the iron oxide and carbon in the sample indicated by XPS, which are in good agreement with the values reported for Fe_3O_4 in the literature [18]. The quantitative analysis indicated the molar presence of carbon (74.71%), oxygen (24.60%) and iron (0.69%) in the nanocomposites.

The XRD pattern of the magnetic particles was presented in Fig. 4. It shows that the diffraction peaks correspond to the (2 2 0), (3 1 1), (4 0 0), (4 2 2) and (4 4 0) suggests the particles could be easily indexed to Fe_3O_4, plus no obvious sharp diffraction peak corresponding to the graphite is present indicating that most of

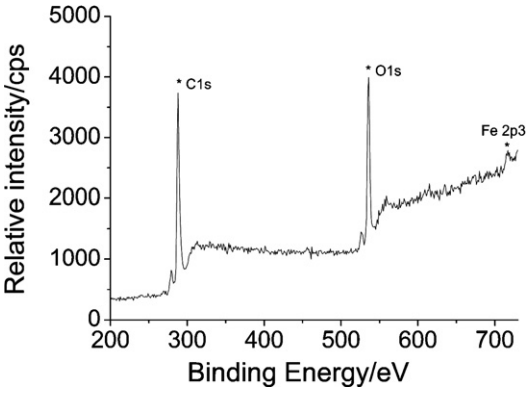

Fig. 3. XPS spectrum of Fe_3O_4/C nanoparticles.

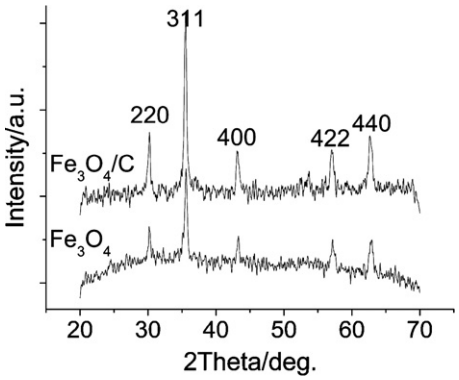

Fig. 4. XRD patterns of Fe_3O_4 and Fe_3O_4/C nanoparticles.

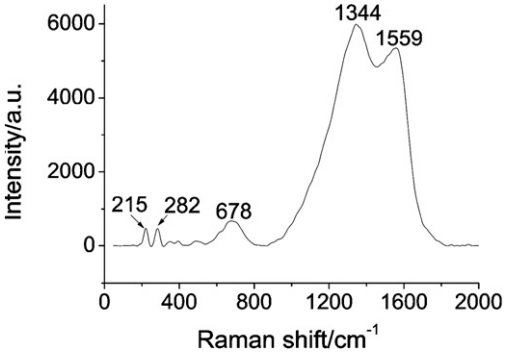

Fig. 5. Raman spectrum of Fe_3O_4/C nanomaterials.

the carbon prepared with this method is amorphous [17,19]. Fig. 5 displays Raman spectra of the Fe_3O_4/C nanomaterials. In low wave number region, there are peaks at 215, 282, 678 cm^{-1}, which are in accordance with that of Fe_3O_4 [18,20,21]. In addition, the two distinct peaks at 1344 and 1559 cm^{-1} can be assigned to the "D" and "G" band of carbon materials [22,23]. That is from the glucose hydrothermal reaction, then coating to the surface of magnetic nanoparticles. Furthermore, the carbonization of glucose during a hydrothermal treatment is due to the cross linking of the intermolecular dehydration products of the glucose, oligosaccharides and/or other macromolecules derived from glucose, according to the previous reports [24]. FTIR spectra is used to analyze the obtained Fe_3O_4/C nanospheres and demonstrates that the strong IR band at 579 cm^{-1} is characteristic of the Fe–O vibrations, the peaks at 1581 cm^{-1} and 1699 cm^{-1} are attributed to C=C and C=O vibrations, and the peak at 3449 cm^{-1} implied the existence of residual hydroxyl groups (Fig. 6) [17,25,26]. Those hydrophilic functional

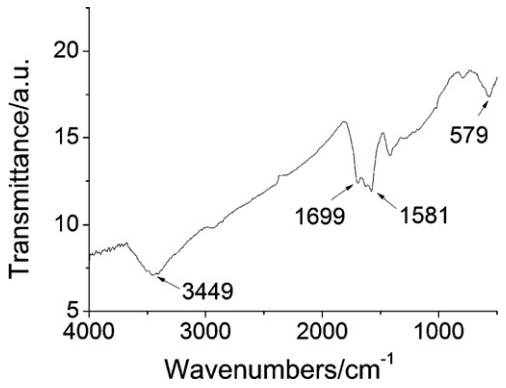

Fig. 6. FTIR spectrum of Fe_3O_4/C nanospheres.

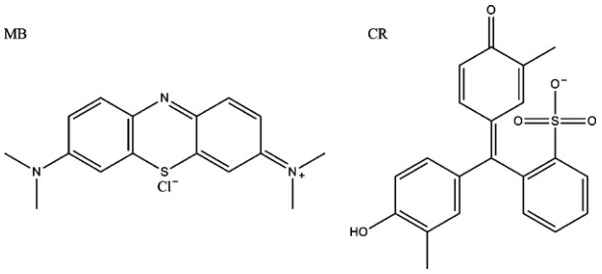

Fig. 7. Chemical structures of MB and CR.

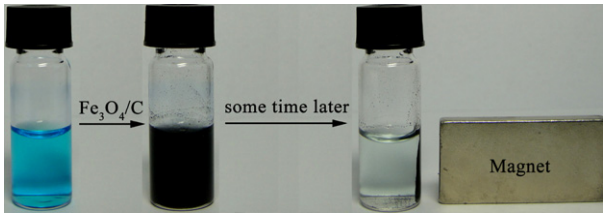

Fig. 8. Photographs of Fe_3O_4/C composites adsorption behavior and magnetic separation phenomenon. Blue solution is MB solution, after mix with Fe_3O_4/C composite a few hours later, magnetic separation by an external magnet can obtain a clear solution.

groups result in the enhanced hydrophilia of the obtained composites.

3.2. Adsorption and removal of dyes from aqueous solution

Dyes removal experiments were carried out by adsorbing MB and CR from aqueous solution and the structures of MB and CR have been displayed in Fig. 7. In the test, Fig. 8 shows the photographs of the Fe_3O_4/C nanomaterials adsorption process. The nanospheres were dispersed in the dye solution firstly, and after a few hours later, attracted and separated by an external magnet easily, then the solution had been mostly purified as shown.

The effect of contact time on the amount of dye adsorbed was investigated at 10 mg L^{-1} initial concentration of both dyes. It can be observed from Fig. 9 that the dye adsorption increases with the increase of treating time, the sample attained about 90% of the adsorption capacity at equilibrium within 2.5 h.

The dye removal percentage was calculated as [1]:

$$\%\text{removal} = \frac{C_0 - C_t}{C_0} \times 100$$

where C_0 and C_t (mg L^{-1}) are the concentration of dye in the solution at initial and equilibrium time, respectively.

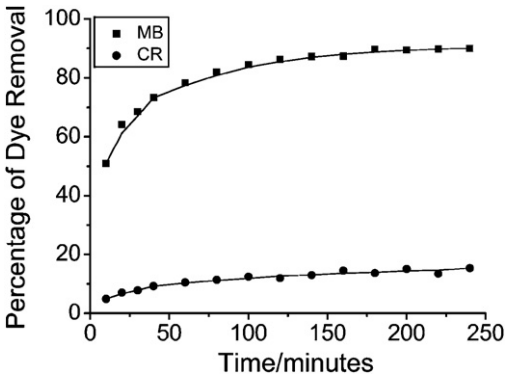

Fig. 9. The effect of contact time on the adsorption of dyes (MB and CR) to Fe_3O_4/C nanomaterials (C_0 = 10 mg L^{-1}).

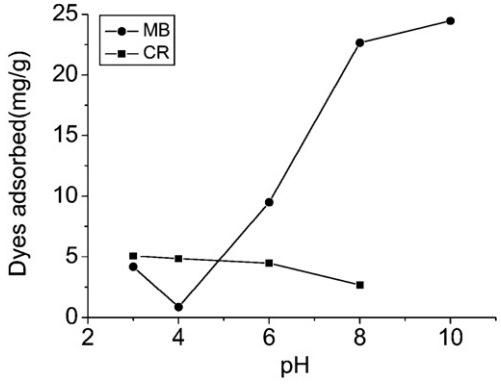

Fig. 10. The effect of pH on the adsorption of dyes to Fe_3O_4/C nanomaterials (C_0 = 10 mg L^{-1}).

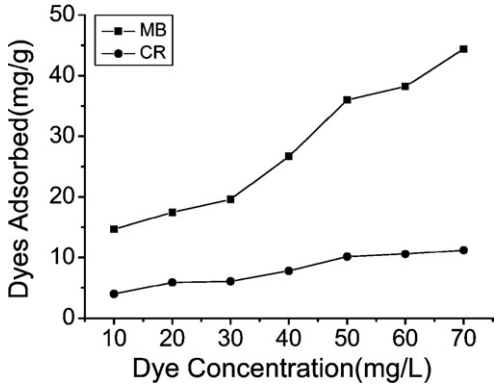

Fig. 11. The effect of different dye equilibrium concentrations to Fe_3O_4/C nanomaterials.

The effect of pH on adsorption of dyes was investigated in Fig. 10 from pH 3 to 10; except for CR was only conducted from pH 3 to 8 for avoiding detection error due to its color change after pH 8. Solution pH may affect both aqueous chemistry and surface binding sites of the adsorbent [6]. For MB, the pH regulates the ionization of both Fe_3O_4/C nanoparticles and MB, so it has significant influence on the adsorption process. Generally, Fe_3O_4/C nanoparticles adsorb more MB at higher pH values, this phenomenon can be explained on the basis of the added the negative charge of the nanomaterials surface, which would enhance the electrostatic interaction of nanomaterials and MB. Similarly, the pH-regulated adsorption behavior is also observed in the studies of other carbon adsorbents [27]. For CR, the observed decrease in the uptake value along with pH valve enhanced from 3 to 8, may be attributed to the Fe_3O_4/C nanoparticles were ionized and had more negative charges, which would enhance the electrostatic repulsion of nanomaterials and negative charged dye (CR). As shown in Fig. 11, the adsorption capacity of MB is higher than CR at all concentration ranges. The maximum adsorption capacities at 298 K in the concentration range studied are 44.38 mg g^{-1} and 11.22 mg g^{-1} for MB and CR, respectively. The amount of dye adsorbed (Q_e) was calculated using the equation [2,28,29]:

$$Q_e = C_0 - C_t \frac{V}{m}$$

where C_0 and C_t are the initial and equilibrium concentrations of dye (mg L^{-1}), m is the mass of Fe_3O_4/C nanomaterials (g), and V is the volume of solution (L).

The higher adsorption capacity for MB may be attributed to those functional groups (such as –OH, C=O) on the composite surface as well as negative potential of the magnetic nanocomposites that provide weak electrostatic interaction between the cationic dye and the nanomaterials.

4. Conclusion

Super paramagnetic Fe_3O_4/C nanoparticles with average size ~250 nm in the diameter have been synthesized for removal of the cationic dyes from water. The prepared magnetic nanospheres can be well dispersed in the aqueous solution and easily separated from the solution in 10 s using an external magnet after adsorption. The adsorption capacities for MB and CR in the concentration range studied are 44.38 mg g^{-1} and 11.22 mg g^{-1} respectively. The process of purifying water pollution presented here is clean and safe using the magnetic nanomaterials. Hence, it provides a simple and environment friendly separation tool for removal of organic dyes or other pollutants.

Acknowledgements

This work was supported by National Science Foundation of China and the Student Science and Technology Innovation Finance Scheme of Fudan University.

References

[1] S. Qadri, A. Ganoe, Y. Haik, Removal and recovery of acridine orange from solutions by use of magnetic nanoparticles , J. Hazard. Mater. 169 (1–3) (2009) 318–323.
[2] S. Qu, F. Huang, S. Yu, G. Chen, J. Kong, Magnetic removal of dyes from aqueous solution using multi-walled carbon nanotubes filled with Fe_2O_3 particles , J. Hazard. Mater. 160 (2–3) (2008) 643–647.
[3] R.D. Ambashta, M. Sillanpää, Water purification using magnetic assistance: a review , J. Hazard. Mater. 180 (1–3) (2010) 38–49.
[4] Y. Liu, S. Guo, Z. Zhang, W. Huang, D. Baigl, M. Xie, Y. Chen, D. Pang, A micropillar-integrated smart microfluidic device for specific capture and sorting of cells , Electrophoresis 28 (24) (2007) 4713–4722.
[5] J. Gong, B. Wang, G. Zeng, C. Yang, C. Niu, Q. Niu, W. Zhou, Y. Liang, Removal of cationic dyes from aqueous solution using magnetic multi-wall carbon nanotube nanocomposite as adsorbent , J. Hazard. Mater. 164 (2–3) (2009) 1517–1522.
[6] L. Ai, H. Huang, Z. Chen, X. Wei, J. Jiang, Activated carbon/$CoFe_2O_4$ composites: facile synthesis, magnetic performance and their potential application for the removal of malachite green from water , Chem. Eng. J. 156 (2) (2010) 243–249.
[7] X. Luo, L. Zhang, High effective adsorption of organic dyes on magnetic cellulose beads entrapping activated carbon , J. Hazard. Mater. 171 (1–3) (2009) 340–347.
[8] B. Zargar, H. Parham, A. Hatamie, Fast removal and recovery of amaranth by modified iron oxide magnetic nanoparticles , Chemosphere 76 (4) (2009) 554–557.
[9] H. Zhu, R. Jiang, L. Xiao, W. Li, A novel magnetically separable [gamma]-Fe_2O_3/crosslinked chitosan adsorbent: Preparation, characterization and adsorption application for removal of hazardous azo dye , J. Hazard. Mater. 179 (1–3) (2010) 251–257.
[10] K.Z. Elwakeel, Removal of Reactive Black 5 from aqueous solutions using magnetic chitosan resins , J. Hazard. Mater. 167 (1–3) (2009) 383–392.

[11] A.A. Atia, A.M. Donia, W.A. Al-Amrani, Adsorption/desorption behavior of acid orange 10 on magnetic silica modified with amine groups , Chem. Eng. J. 150 (1) (2009) 55–62.
[12] V. Rocher, J. Siaugue, V. Cabuil, A. Bee, Removal of organic dyes by magnetic alginate beads , Water Res. 42 (4–5) (2008) 1290–1298.
[13] V. Rocher, A. Bee, J. Siaugue, V. Cabuil, Dye removal from aqueous solution by magnetic alginate beads crosslinked with epichlorohydrin , J. Hazard. Mater. 178 (1–3) (2010) 434–439.
[14] L. Wang, J. Bao, L. Wang, F. Zhang, Y. Li, One-pot synthesis and bioapplication of amine-functionalized magnetite nanoparticles and hollow nanospheres , Chem. Eur. J. 12 (24) (2006) 6341–6347.
[15] H. Deng, X. Li, Q. Peng, X. Wang, J. Chen, Y. Li, Monodisperse magnetic single-crystal ferrite microspheres , Angew. Chem. Int. Ed. 44 (18) (2005) 2782–2785.
[16] D. Qi, J. Lu, C. Deng, X. Zhang, Magnetically responsive Fe_3O_4@C@SnO_2 core–shell microspheres: synthesis, characterization and application in phosphoproteomics , J. Phys. Chem. C 113 (36) (2009) 15854–15861.
[17] Z. Zhang, H. Duan, S. Li, Y. Lin, Assembly of magnetic nanospheres into one-dimensional nanostructured carbon hybrid materials , Langmuir 26 (9) (2010) 6676–6680.
[18] F. Cao, C. Chen, Q. Wang, Q. Chen, Synthesis of carbon-Fe_3O_4 coaxial nanofibres by pyrolysis of ferrocene in supercritical carbon dioxide , Carbon 45 (4) (2007) 727–731.
[19] H. Niu, S. Zhang, X. Zhang, Y. Cai, Alginate-polymer-caged, C18-functionalized magnetic titanate nanotubes for fast and efficient extraction of phthalate esters from water samples with complex matrix , ACS Appl. Mater. Interfaces 2 (4) (2010) 1157–1163.
[20] S. Ni, X. Wang, G. Zhou, F. Yang, J. Wang, D. He, Designed synthesis of wide range microwave absorption Fe_3O_4-carbon sphere composite , J. Alloys Compd. 489 (1) (2010) 252–256.
[21] O.N. Shebanova, P. Lazor, Raman study of magnetite (Fe_3O_4): laser-induced thermal effects and oxidation , J. Raman Spectrosc. 34 (11) (2003) 845–852.
[22] T. Kohn, K.J.T. Livi, A.L. Roberts, P.J. Vikesland, Longevity of granular iron in groundwater treatment processes: corrosion product development , Environ. Sci. Technol. 39 (8) (2005) 2867–2879.
[23] H.I. Hima, X. Xiang, L. Zhang, F. Li, Novel carbon nanostructures of caterpillar-like fibers and interwoven spheres with excellent surface super-hydrophobicity produced by chemical vapor deposition , J. Mater. Chem. 11 (2008) 1245–1252.
[24] C. Yao, Y. Shin, L. Wang, C.F. Windisch, W.D. Samuels, B.W. Arey, C. Wang, W.M. Risen, G.J. Exarhos, Hydrothermal dehydration of aqueous fructose solutions in a closed system , J. Phys. Chem. C 111 (42) (2007) 15141–15145.
[25] X. Sun, Y. Li, Colloidal carbon spheres and their core/shell structures with noble-metal nanoparticles , Angew. Chem. Int. Ed. 43 (5) (2004) 597–601.
[26] V.G. Pol, L.L. Daemen, S. Vogel, G. Chertkov, Solvent-free fabrication of ferro-magnetic Fe_3O_4 octahedra , Ind. Eng. Chem. Res. 49 (2) (2010) 920–924.
[27] S. Yang, S. Chen, Y. Chang, A. Cao, Y. Liu, H. Wang, Removal of methylene blue from aqueous solution by graphene oxide , J. Colloid Interface Sci. 359 (1) (2011) 24–29.
[28] B. Saha, S. Das, J. Saikia, G. Das, Preferential and enhanced adsorption of different dyes on iron oxide nanoparticles: a comparative study , J. Phys. Chem. C 115 (16) (2011) 8024–8033.
[29] L.J. Kennedy, J.J. Vijaya, G. Sekaran, K. Kayalvizhi, Equilibrium, kinetic and thermodynamic studies on the adsorption of m-cresol onto micro- and mesoporous carbon , J. Hazard. Mater. 149 (1) (2007) 134–143.